Publication II

Juha T. Toivanen, Tommi A. Laitinen, Sergey Pivnenko, and Lasse Nyberg. 2009. Calibration of multi-probe antenna measurement system using test zone field compensation. In: Proceedings of the 3rd European Conference on Antennas and Propagation (EuCAP 2009). Berlin, Germany. 23-27 March 2009. Pages 2916-2920. ISBN 978-3-00-024573-2.

Calibration of Multi-Probe Antenna Measurement System Using Test Zone Field Compensation

Juha T. Toivanen[#1], Tommi A. Laitinen[#2], Sergey Pivnenko[*3], Lasse Nyberg[#4]

[#]*Department of Radio Science and Engineering, Helsinki University of Technology*
PL 3000, 02015 TKK, Finland
[1]juha.toivanen@tkk.fi

[*]*Department of Electrical Engineering, Technical University of Denmark*
Ørsteds Plads, bldg. 348, DK-2800 Kgs. Lyngby, Denmark
[3]sp@elektro.dtu.dk

***Abstract*— A new method for calibrating a multi-probe antenna measurement system is presented. The method is based on a modification of the test zone field compensation technique [1]. First experiments with the technique on a multi-probe range are presented, and they show accuracy comparable to that of a traditional measurement using the cable calibration.**

I. Introduction

Multi-probe antenna measurement systems are nowadays widely used, especially in characterizing the radiation properties of small antennas. These systems provide clear advantages in terms of measurement speed, as compared with the traditional single-probe systems. There are, however, also some difficulties specific to such systems. Among these are the more complicated system calibration and the deterioration of the anechoic properties of the measurement chamber due to the large number of probe antennas.

The calibration of a multi-probe system requires one to determine the response of each measurement channel to be able to compensate for the channel differences during the processing of the measurement data. One way to perform this calibration is to detach each measurement probe and measure the S_{21} response of each measurement channel using a vector network analyser (cable calibration). This kind of calibration is a very time-consuming process and, furthermore, does not take into account the differences in the probe responses nor the range reflections. Another possibility is to use a reference radiator, which is pointed towards each of the probes, while measuring the channel response [2]. This calibration includes the probe responses, but still does not address the problem of signal reflections within the measurement chamber.

The purpose of this paper is to present and demonstrate an alternative calibration method for multi-probe systems. The method is a modification of the test zone field compensation technique [1], [3]. It is perhaps best understood by considering each probe as transmitting a signal that produces a certain incoming field, called the test zone field (TZF), in the location of the antenna under test (AUT). The TZF induced by each probe is determined through measurements with a known calibration antenna. The information on the channel responses, including the reflected and scattered fields is then contained in the TZFs and can be used for system calibration.

In this paper, first tests of the TZF calibration method on a multi-probe range at the Helsinki University of Technology (TKK) are reported. The TZF calibration is contrasted with a traditional cable calibration procedure. It is shown that both methods provide comparable measurement accuracy. The accuracy of the TZF calibration method depends on the uncertainties in the TZF measurement.

II. Theoretical Background

The TZF calibration method is based on the spherical-wave theory. It consists of essentially two phases, both of which utilize the transmission formula [4]

$$w_t(\varphi,\theta,\chi) = \sum_{s\mu nm} Q_{s\mu n} e^{i\mu\varphi} d^{n}_{m\mu}(\theta) e^{im\chi} R_{smn} . \qquad (1)$$

This formula gives the signal w_t received by an antenna (with receiving coefficients R_{smn}) placed in a test zone in an orientation given by the angles φ, θ *and* χ. The $Q_{s\mu n}$ are the coefficients of the test zone incident field and d is the spherical-wave rotation function.

In the first phase, the $Q_{s\mu n}$ of the TZF corresponding to each probe signal, are determined by measuring w_t as a function of the orientation of a calibration antenna (TZF probe) in the test zone. The R_{smn} of the TZF probe must be known from a separate calibration measurement. Then, using eqn. (1), a system of linear equations is formed and solved for the $Q_{s\mu n}$ using e.g. a generalized matrix inverse.

The second phase is the actual antenna measurement. The TZF information is contained in the $Q_{s\mu n}$, which are different for each probe. The signal w_t received by the AUT is measured using a sufficient number of AUT orientations, depending on the multi-probe system. Again, a system of linear equations is formed using eqn. (1), the only difference being that this time the unknown parameters are the R_{smn} of the AUT. Solving for R_{smn} then gives the calibrated measurement result since the radiated electric field of the AUT is given by

$$\overline{E}(r,\theta,\varphi) = \sum_{smn} vT_{smn}\, \overline{F}^{(3)}_{smn}(r,\theta,\varphi) \ , \qquad (2)$$

where v is the input signal, F_{smn} are the outgoing spherical vector wave functions and the T_{smn} are the AUT transmission coefficients, related to the receiving coefficients as

$$T_{smn} = (-1)^m R_{s,-m,n}. \quad (3)$$

An important point to consider is that using a matrix-inverse solution method in the second phase instead of the more traditional Fourier-transform-based method (used in [1]) provides several advantages. First, the solution is obtained directly; no iterations are required. Second, there are no limitations on the amplitude of the range reflections. This means that, in principle, the TZF calibration technique, as presented here, can be used in a measurement chamber without any anechoic properties i.e. without RF absorbers (it does not, however, compensate for multiple reflections between the AUT and the probes). Third, it is not necessary to use a measurement point grid that is regular in θ and φ. Instead, the measurement point locations can be chosen, e.g., to provide a uniform distribution over a spherical surface with no point clustering near the poles.

The downside of this solution method is that it is computationally demanding and potentially more sensitive to errors in the measurement data due to the matrix-inverse operation. The number of spherical modes $J = 2N(N+2)$ depends on the truncation number N of the mode series, which in turn is proportional to the test zone size ($N \sim kr_0$). The radius of the test zone (r_0) must be large enough to enclose the AUTs to be tested. Hence, as the electrical size of the AUT increases, the number of spherical modes required for the characterization of the AUT and test zone fields expands rapidly. This directly influences the size of the matrix and the computational requirements in the matrix inversion. However, simulations ([3]) and measurements presented in this paper show that this method is useful at least with small antennas, having sizes in the order of few wavelengths.

III. Test Setup and Measurements

The measurements were performed at the Department of Radio Science and Engineering in the Helsinki University of Technology. Prior to this, the radiation characteristics of the TZF probe and the AUTs (for reference purposes) were measured in the DTU-ESA Spherical Near-Field Antenna Test Facility, located in the Technical University of Denmark. The antennas and the calibration procedure are described in the following sections.

A. Test Zone Field Probe

The TZF probe must be selected so that it is sensitive for a large-enough number of spherical modes, considering the subsequent characterization of the AUTs. In practice this means that it should be larger than the AUTs, or, if it is smaller, it must be located away from the centre of rotation during the calibration measurement.

The probe selected for these measurements is shown in Fig. 1. It is a wideband Vivaldi-type printed-circuit-board element located within the tube protruding out from the circular absorber sheet. The absorber collar is used in order to reduce the back-lobe radiation of the probe. The probe holder incorporates rotary joints so that the polarization of the probe can be changed by rotating the tube.

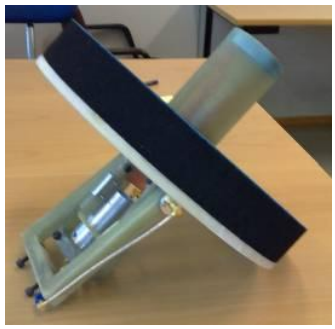

Fig. 1. The TZF probe.

Fig. 2 presents the spherical-mode spectrum of the TZF probe at 1.6 GHz. The spherical mode number in the horizontal axis corresponds to the j-notation, whereby the spherical mode index triplet (s,m,n) is converted into the single index j, defined as [4]

$$j = 2\{n(n+1) + m - 1\} + s, \quad (4)$$

where the integer indices get the values $s = \{1, 2\}$, $n = \{1 \ldots N\}$, $m = \{-n \ldots n\}$ and $j = \{1 \ldots J\}$. It can be seen from Fig. 2 that some modes corresponding to $N = 7$ (i.e. the interval $97 \leq j \leq 126$) are attenuated less than 8 dB compared with the highest modes. After this, the modes attenuate rapidly.

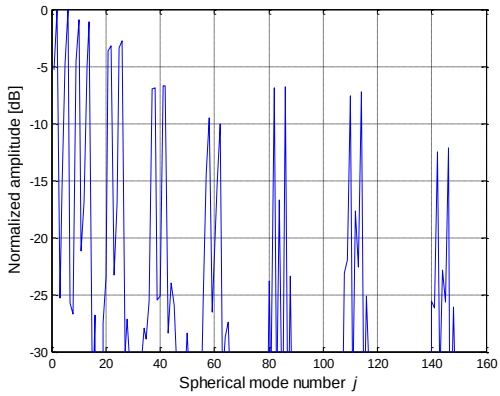

Fig. 2. The spherical mode spectrum of the TZF probe at 1.6 GHz.

B. Reference AUTs

The first AUT is a diversity antenna prototype operating at 1.6 GHz, with dimensions 43x107x9 mm^3 [5]. This antenna is shown in Fig. 3, where the two radiating elements can be seen in the upper left and right corners. These elements are labelled AUT1 and AUT2. This antenna was chosen for the

measurements as an example of a realistic communications device antenna. An ordinary dipole antenna was chosen as AUT3. It operates at 1.8 GHz

Both of the AUTs are relatively small in wavelengths. This means their spherical-mode spectrum does not extend very far and the selected TZF probe is certainly large enough in comparison so that the required modes can be resolved. Due to the small size of the AUTs and the relatively small number of probes (see next section), a truncation number of $N = 3$ was used in the measurements.

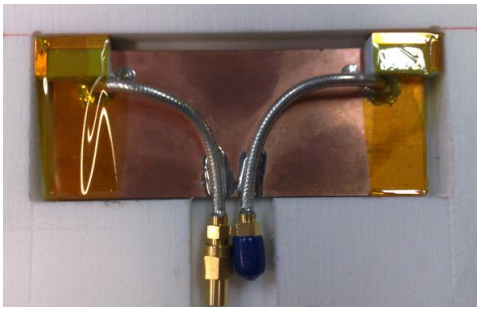

Fig. 3. The diversity antenna prototype (AUT1 & AUT2).

C. Test Zone Field Calibration

The measurements were performed with the multi-probe system presented in [6] and [7]. This system consists of 32 dual-polarized probes that are spread uniformly over a spherical surface. The test zone is located in the centre of the sphere. The TZF measurement set-up is shown in Fig. 4, where the TZF probe can be seen in the middle and the measurement probes around it, pointing towards the centre. The TZF probe was installed on a rotating arm, which enabled a full 360-degree azimuth scan. Elevation scan was made possible by the probe holder (see Fig. 1).

The required number of measurement points in the calibration measurement is determined by the number of significant spherical modes of the TZF probe. The mode series must be truncated appropriately. If the selected truncation number is too low, one runs into aliasing problems and if it is too high, the computational complexity of the problem increases unnecessarily. In the data analysis it was found that a good point for the truncation is the point where the cumulative power content of the modes exceeds 98% of the total power. For example, at 1.6 GHz this means that a truncation number of $N = 7$ is used, giving $J = 126$ modes (see Fig. 2).

The number of measurement points should be somewhat higher than the number of modes. In the calibration measurement, a 20-degree step was chosen for both θ and φ and the measurement was performed in two polarizations, giving 292 measurement points in total. At the operating frequency of the dipole (1.8 GHz) the required number of modes, using the above-mentioned criterion, was $J = 160$. Therefore, the oversampling factor was approximately 1.8.

For every orientation of the TZF probe, a full measurement was performed, with each probe at a time measuring the signal transmitted by the TZF probe (due to reciprocity, this is the same as considering the measurement probes as transmitters and the TZF probe as the receiver). This way, enough data was gathered for the characterisation of the TZF corresponding to each and every measurement probe. Although the total amount of data is very large, one should bear in mind that this calibration is valid as long as there are no significant changes in the system or in the measurement environment, and the obtained calibration data can be used for all AUTs that fit within the characterised test zone. Furthermore, when performed manually, as was done here, the calibration measurement is very time-consuming, but when automated with an appropriate positioner system, it becomes easy to perform.

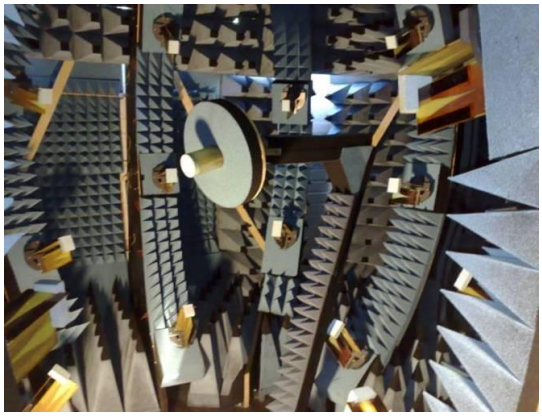

Fig. 4. Measurement of the TZF. The TZF probe is measured in different orientations in the test zone.

D. AUT measurement

After the TZF measurement, all the AUTs were measured by placing them in the centre of the test zone and recording the signal received by each measurement probe. The AUTs were measured in a single orientation. Due to the small size of the AUTs and the three-dimensional measurement probe configuration, sufficient measurement data was obtained without AUT rotation.

IV. Test Results

In this section, the results of the tests are presented. The measurements performed at TKK using both the TZF calibration and the cable calibration are compared to the reference measurements performed at the DTU-ESA facility.

A. Directivity and Total Radiated Power

The parameter of interest in small-antenna measurements is often the directivity of the antenna. Small antennas typically have omni-directional characteristics so there is no definitive main-lobe direction. Also, in the case of mobile terminals, for example, the base station may be located in any direction

relative to the antenna. Therefore, all directions can be considered equally important when measuring small antennas.

The results of the measurements are presented in terms of the normalized directivity error, calculated as a function of direction for the full space angle as

$$\Delta D(\theta,\phi) = \frac{D_{meas}(\theta,\phi) - D_{true}(\theta,\phi)}{\max(D_{true})} \quad , \tag{5}$$

where D_{true} is taken to be the reference value measured at the DTU-ESA facility. Table 1 presents the RMS values of ΔD for measurements with both the TZF calibration (ΔD_{TZF}) and the cable calibration ($\Delta D_{\mathrm{CABLE}}$). The RMS values have been calculated from 106 samples distributed uniformly around the AUT. The results show that the performance of the two calibration methods is approximately the same. The normalized directivity error is in the range of 0.5 to 0.8 dB (at pattern maximums) in all measurements. A representative pattern cut in Fig. 5 shows the DTU-ESA reference measurement of AUT1 directivity compared with the TKK measurement using both the TZF calibration and the cable calibration.

TABLE I
NORMALIZED DIRECTIVITY ERRORS FOR MEASUREMENTS WITH THE TZF CALIBRATION AND THE CABLE CALIBRATION

AUT	Frequency [GHz]	RMS Directivity Error [dB]	
		ΔD_{TZF}	$\Delta D_{\mathrm{CABLE}}$
AUT1	1.6	0.6	0.5
AUT2	1.6	0.7	0.8
AUT3	1.8	0.8	0.7

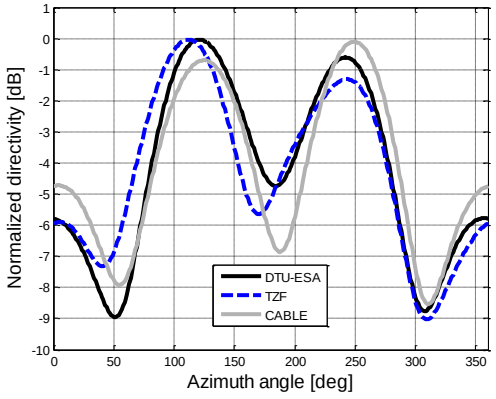

Fig. 5. A representative pattern cut for AUT1, showing the DTU-ESA reference measurement and the TKK measurement with TZF and cable calibration.

Another figure of merit that is often used is the radiation efficiency of the AUT. The efficiency can be calculated from total radiated power (TRP) measurements and is typically determined by comparing the TRP of the AUT to the TRP of a reference antenna with known efficiency. Therefore, a reference measurement is required. In the case of TZF calibration, the TZF measurement directly provides this reference, assuming the radiation efficiency of the TZF probe is known. With the TZF calibration, the errors in the measured efficiency values were less than 0.6 dB for all AUTs compared with the DTU-ESA measurement.

B. Measurement Uncertainties

The uncertainties in the TZF measurement are the main determinant of the accuracy of the TZF calibration method. During the TZF measurement, a control measurement was performed at regular intervals with the TZF probe in a pre-determined reference position. The standard deviation of these measurement values gives some indication on the overall measurement uncertainty. It was typically below 1 dB (normalized to maximum value), depending on the measurement probe and the frequency. This uncertainty is quite high and is possibly caused by the large attenuation in the measurement path.

Another source of uncertainty was the back lobe radiation of the TZF probe. Even though the measurements performed for the TZF probe at the DTU-ESA measurement range provided otherwise highly accurate data, the back lobe could not be measured reliably. This was due to obstruction from the tower, where the TZF probe was installed during the measurement. The back lobe radiation was noticed during the measurements at TKK and the problem became worse at lower measurement frequencies (the TZF probe was measured at a wide range of 0.4-4 GHz). However, around the 1.6-1.8 GHz range this problem was not so severe.

In retrospect, the design of the TZF probe support arm (see Fig. 4) should have been different. With the present design, the arm is located very close to some of the measurement probes during the TZF measurement and the signals corresponding to these probes are scattered from the arm. Since the arm is not present during the actual AUT measurements, this could be a significant source of error.

V. CONCLUSION

An alternative calibration method for multi-probe antenna measurement systems has been presented. The method provides channel balance calibration and, in addition, compensation for the reflected and scattered signals (excluding multiple reflections between the AUT and the probes) that are present in the measurement chamber.

The method is best applicable for measurement of small antennas, with maximum dimensions of a few wavelengths or less. With larger antennas, the computational requirements increase rapidly. The calibration accuracy is proportional to the uncertainties in the TZF measurement. The results presented in this paper show that performance similar to traditional calibration methods can be achieved. Furthermore, the method has the potential to be used also in non-anechoic environments with high levels of signal reflections.

ACKNOWLEDGMENT

The Academy of Finland is thanked for funding this research. NordForsk is thanked for financial support of the

work which allowed accurate reference measurements to be performed in the DTU-ESA Spherical Near-Field Antenna Test Facility.

REFERENCES

[1] D.N. Black, E.B. Joy, "Test zone field compensation," *IEEE Transactions on Antennas and Propagation*, vol. 43, pp. 362–368, 1995.

[2] P. Garreau, L. Duchesne, A. Gandois, L. Foged, P. O. Iversen, "Probe array concepts for fast testing of large radiating structures," in *Proc. AMTA2004*, 2004, pp. 159-164.

[3] J.T. Toivanen, T.A. Laitinen, "Small-antenna measurements in non-anechoic environments," submitted to *Electronics Letters*.

[4] J.E. Hansen, Ed., *Spherical Near-Field Antenna Measurements*, London, UK: Peter Peregrinus Ltd., 1988.

[5] M. Mustonen, "Multi-element antennas for future mobile terminals," Lic. Sc. thesis, Helsinki University of Technology, Espoo, Finland, May 2008.

[6] T.A. Laitinen, J. Toivanen, C. Icheln, P. Vainikainen, "Spherical measurement system for determination of complex radiation patterns of mobile terminals," *Electronics Letters*, vol. 40, no. 22, pp. 1392–1394, 2004.

[7] J. Toivanen, T. A. Laitinen, C. Icheln, P. Vainikainen, "Spherical wideband measurement system for mobile terminal antennas," in *Proc. 2nd IASTED Int. Conf. Antennas, Radar and Wave Propagation*, 2005, pp. 360-365.